Time-domain model for spherical wave reflection in a flat surface with absorber character – Application to the SOPRA measurement method

Citation for the original published paper (version of record):
Waaranperä, M., Forssén, J. (2025). Time-domain model for spherical wave reflection in a flat surface with absorber character –
Application to the SOPRA measurement method. Applied Acoustics, 227.
http://dx.doi.org/10.1016/j.apacoust.2024.110251

Applied Acoustics 227 (2025) 110251

Contents lists available at ScienceDirect

Applied Acoustics

journal homepage: www.elsevier.com/locate/apacoust

Time-domain model for spherical wave reflection in a flat surface with absorber character – Application to the SOPRA measurement method

Monica Waaranperä *, Jens Forssén

Division of Applied Acoustics, Department of Architecture and Civil Engineering, Chalmers University of Technology, SE-412 96 Gothenburg, Sweden

ARTICLE INFO

Keywords:
Road noise barrier
Direct sound field
Sound reflection index measurement
Time-domain modelling
Direct field absorption model
SOPRA method

ABSTRACT

This paper presents a developed time-domain model for the reflection of spherical waves in an absorber-like surface. The model is made to enable evaluation of measurement methods for assessing the sound absorptive properties of traffic noise barriers in direct sound field, it is thus called the Direct Field Absorption (DFA) model. In this study, the DFA model is applied to the in-situ SOPRA method for quick sound reflection index measurements on road noise barriers. The DFA model results in an impulse response (IR), based on a theoretically derived impedance of a certain absorber. The DFA IR is entered to the SOPRA formula to calculate the reflection index, RI_Q, of the absorber, which is subsequently compared to the measured RI_Q of a wall fitted with the absorber in question. If the results are similar, it is reasonable to assume that the SOPRA measurement results are valid. But if there are any significant differences between the DFA and SOPRA sound reflection indices, possible reasons for them should be examined.

The first results are encouraging, showing that the DFA model can be a valuable tool to evaluate the results of reflection measurements. Furthermore, the DFA model could be useful for estimating the sound absorptive performance at lower frequencies of a noise barrier limited to its spatial extent in width and height, i.e., when it is physically impossible to measure. Further studies are necessary though, since the conclusions of this paper are based on only one kind of absorber.

1. Introduction

Sound absorptive noise barriers are often installed along roads where sound reflections could increase the sound levels on the opposite side of the roads, or along railways to reduce the risk of deterioration due to sound reflections between the trains and noise barriers. The sound absorbing performance of an industrially manufactured noise barrier is in general tested in laboratory under diffuse sound field conditions, according to the standards EN 1793-1 for road noise barriers [1] and EN 16272-1 for railway noise barriers [2]. However, it is not always tested under direct sound field conditions, like the non-reverberant situations in-situ along roads and railways in open terrain, with the corresponding standards to measure the sound reflection, EN 1793-5 [3] and EN 16272-5 [4], respectively. (It can be noted that the test standards for sound insulation in diffuse or direct sound field are: EN 1793-2 [5] and EN 1793-6 [6], respectively, for road noise barriers and EN 16272-2 [7] and EN 16272-6 [8], respectively, for railroad noise barriers.)

Moreover, in Sweden, a large number of the installed noise barriers are built on-site and thus not tested according to any noise barrier standard at all. The intrinsic performance of these noise barriers is rarely controlled in-situ, as long as the resulting sound levels at the receivers meet the required single-number, A-weighted noise limit values (e.g., $LA_{eq,24h}$ values in dB).

To measure the intrinsic acoustic performance of both new and older installed noise barriers, with or without declared sound absorbing or sound insulating properties, the EN standard methods for direct sound field could be used, but they require meticulous set-up and handling of the equipment, which is quite time consuming. The need for an easier way to investigate the acoustic function of installed noise barriers is the reason for the development of the “quick methods”, a.k.a. the SOPRA methods, which are both faster and in some parts simplified versions of the EN 1793-5 and the EN 1793-6. The SOPRA methods have been developed over many years, including validations and updates, e.g., in recent papers [9–13]. It must be stressed, though, that the SOPRA methods cannot replace the full standard methods for declaring the acoustic characteristics of certain products.

Whether the in-situ sound reflection index measurements are performed with the standard or the SOPRA methods, restricted time and accessibility on the road sites may limit the number of measured sec-

* Corresponding author.
E-mail address: monicaw@chalmers.se (M. Waaranperä).

https://doi.org/10.1016/j.apacoust.2024.110251
Received 26 June 2024; Received in revised form 10 August 2024; Accepted 20 August 2024
Available online 30 August 2024

tions of a noise barrier, resulting in less data for assessing the quality of the results from the measurements.

To enable evaluation or prediction of the outcome of direct field sound reflection measurements, the Direct Field Absorption (DFA) model has been developed, a time-domain model for the reflection of spherical waves in an absorber-like surface. The time-modelling approach is preferred since a central part of reflection measurement methodology is to estimate the time signal at a receiver as due to an impulse emitted from the source, i.e., to estimate the impulse-response function (IR). The estimated IR enables the removal of unwanted late parts, e.g., originating from sound reflections in the ground.

The main focus of the present paper is the application of the DFA model for evaluating the results of the in-situ SOPRA method for quick sound reflection index (RI_Q) measurements on road noise barriers, since the method, so far, only is developed for road side barriers, referring to the EN 1793-5. But technically, the SOPRA method could be used for reflection measurements on rail noise barriers as well, with references to the corresponding parts of the standard EN 16272-5 instead. The DFA model for creating impulse responses from sound absorbing surfaces would function for either purpose.

The paper is organised as follows: The method description in Section 2 comprises the development of the DFA model (Section 2.1) and a summary of the SOPRA quick sound reflection index measurement method (Section 2.2). Section 3 shows an example of the application of the DFA model for evaluating the results of a SOPRA measurement. Section 4 concludes the paper, including plans for future work with the DFA model.

2. Method

2.1. Modelling approach

The description of the modelling approach at first concerns the frequency-domain modelling of the reflection of a spherical wave in a flat surface described by its impedance, as known from literature. The impedance plane is assumed to be locally reacting, i.e. that the sound waves inside the material are modelled as propagating in normal direction to the surface. Thereafter comes the description of how to model the surface impedance using impedance models based on material properties, using measured data as input. From these parts, the frequency-domain response due to an omnidirectional point source and a reflecting impedance plane can be calculated. It is described how this can be made and thereafter how to find the corresponding impulse responses in time-domain that mimic those of the measurement.

2.1.1. Modelling of spherical wave reflection in an impedance surface

According to the work by Chien and Soroka [14], the velocity potential, ϕ, for the reflected spherical wave from a normally reacting surface can be written (with the time factor $e^{j\omega t}$ suppressed):

$$\phi = [R_{pl} + (1 - R_{pl})F(\xi)]\frac{e^{-jk_0R_2}}{4\pi R_2}. \quad (1)$$

Here, R_{pl} is the plane-wave reflection factor,

$$R_{pl} = \frac{\cos\theta - \beta}{\cos\theta + \beta} \quad (2)$$

where β is the normalised admittance at the surface and θ is the angle of incidence; k_0 is the wave number in air, with $k_0 = \omega/c_0$, where ω is the angular frequency and c_0 is the sound speed in air. The geometry is depicted in Fig. 1, where R_1 and R_2 are the distances travelled by the direct and the reflected waves, respectively. The corresponding direct wave can be written as:

$$\phi_d = \frac{e^{-jk_0R_1}}{4\pi R_1}. \quad (3)$$

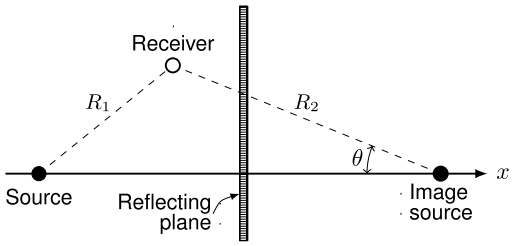

Fig. 1. Geometry with source, image source, receiver, reflection angle, θ, and the reflecting plane with properties defined by the normalised admittance, β.

The spherical reflection factor, Q, may be defined from Eq. (1) as

$$Q = R_{pl} + (1 - R_{pl})F(\xi). \quad (4)$$

The effect of the wave being spherical, compared to a plane wave, can be seen to enter for non-zero values of the function $F(\xi)$, which can be written as

$$F(\xi) = 1 - j\sqrt{\pi}\xi e^{-\xi^2}\mathrm{erfc}(j\xi). \quad (5)$$

Here, ξ is the so-called numerical distance, calculated as

$$\xi = \frac{1}{2}(1 - j)\sqrt{k_0R_2}(\cos\theta + \beta) \quad (6)$$

to ensure the choice of the correct root [15], and $\mathrm{erfc}(\cdot)$ is the complementary error function extended for complex arguments, defined as

$$\mathrm{erfc}(x) = \frac{2}{\pi}\int_x^\infty e^{-t^2}dt. \quad (7)$$

The formulations in Eqs. (1) and (2) are for the velocity potential; however, since the sound pressure, p, differs only by a constant in the frequency-domain notation, i.e. $p = -\rho_0\frac{\partial\phi}{\partial t} = -j\omega\rho_0\phi$, where ρ_0 is the density of air, Eq. (4) is equally valid for the pressure, p as for the velocity potential, ϕ.

For the situations of interest here, the reflection angle is not close to $\pi/2$, for which case the assumptions and approximations behind the above formulation of the spherical reflection are stated to provide adequate results in terms of total level for the sum of direct and reflected waves if also $k_0R_2 \gg 1$ is fulfilled [14]. It is here assumed that sufficient accuracy is obtained also for the reflected wave on its own, provided that $k_0R_2 \gg 1$ and θ is not close to $\pi/2$. The numerical solution of the function $F(\xi)$ is made according to [16].

2.1.2. Impedance modelling of absorber material

Impedance models for porous absorbers based on best fit with measured data may give physically incorrect outcomes, e.g. in terms of negative real part of the effective density at low frequencies, as pointed out by Kirby [17]. Therefore it may be preferable to transition to a physically-based impedance model at low frequencies, e.g. as according to Mechel [18]. As described by Kirby [17], models with known problems at low frequencies include the ones by Delany and Bazely, by Miki and by Komatsu, whereas models by Kirby and Cummings and by Wilson are suggested as relatively straightforward models to use instead [17]. In our case we tested the full-frequency models by Mechel and by Wilson but it turned out that they could not capture the mid-frequency (400–2000 Hz) shape of the absorption coefficient for our samples of 50 mm mineral wool with hard backing. Instead, the model by Miki [19] (and similarly the model by Delany and Bazely) could be made to acceptably fit the mid-frequency shape of the absorption coefficient (as further detailed below), and the Miki model was chosen to be used from here and onwards.

The normalised impedance, Z, according to the Miki model [19] can be written as

$$Z = 1 + 5.5\left(\frac{1000f}{\sigma}\right)^{-0.632} - \mathrm{j}8.43\left(\frac{1000f}{\sigma}\right)^{-0.632} \tag{8}$$

with the corresponding wave number, k, as

$$k = k_0\left[1 + 7.81\left(\frac{1000f}{\sigma}\right)^{-0.618} - \mathrm{j}11.41\left(\frac{1000f}{\sigma}\right)^{-0.618}\right]. \tag{9}$$

where σ is the flow-resitivity. (Concerning the units, we use σ in Ns/m^4, whereas if kNs/m^4 is used, as in [19], the factor 1000 in Eqs. (8) and (9) is removed.) To normalise the impedance, it is divided by the characteristic impedance of air, $Z_0 = \rho_0 c_0$, such that $Z = 1/\beta$, where β is the normalised admittance. In the following, the porous layer is assumed to be placed on a rigid backing, modelled as

$$Z_{\mathrm{RB}} = -\mathrm{j}Z\cot(kd) \tag{10}$$

where d is the layer thickness. The modelled reflection factor for plane waves, R_{pl}, is given by $R_{\mathrm{pl}} = (Z_{\mathrm{RB}} - 1)/(Z_{\mathrm{RB}} + 1)$ and the corresponding absorption coefficient, α_{pl}, is $\alpha_{\mathrm{pl}} = 1 - |R_{\mathrm{pl}}|^2$.

2.1.3. Measuring the impedance of the absorber

As input to the impedance modelling described above, measured impedance data were obtained for a 50 mm thick sample of mineral wool on hard backing using the standardised transfer-function method with an impedance tube [20]. The mineral wool absorber, from which the test samples were cut, had been treated with a pigmented surface layer of glass fibre. For the setup used, the tube diameter is $D = 0.1$ m and the two microphones are separated by $s = 0.05$ m along the tube, with the one furthest away located 0.265 m from the test specimen. The lower frequency limit, f_l, is determined from the condition that s shall exceed 1.5% of the wavelength, λ [20]. In our case, the limit occurs at about 100 Hz and $f_l = 160$ Hz was chosen. The limiting condition for the upper frequency, f_u, becomes $0.45c_0/D \approx 2$ kHz (with $c_0 = 344$ m/s for our lab condition). Based on this, the one-third octave bands 160–2000 Hz were included in the analysis.

The transfer function of the pressure amplitudes (in frequency domain) between the two microphone positions, H_{12}, was measured using a SQuadriga III analyser [21] with a pink noise signal to the loudspeaker; a sampling frequency of 12 kHz was chosen and averaging was made during 30 s for each microphone position with an FFT size of 2^{14} samples. The measurement was repeated for two samples of the mineral wool, repeated twice for each sample, thus providing four datasets for the further analysis.

The measured transfer function, H_{12}, is used to estimate the reflection factor, r, at the surface of the test specimen according to

$$r = \mathrm{e}^{2\mathrm{j}k_0 x_1}\frac{H_{12} - \mathrm{e}^{-\mathrm{j}k_0 s}}{\mathrm{e}^{\mathrm{j}k_0 s} - H_{12}} \tag{11}$$

from which the impedance is estimated as $Z = (1 + r)/(1 - r)$ and the absorption coefficient, α, is estimated as $\alpha = 1 - |r|^2$ [20].

By using the measured absorption coefficient together with the model for α_{pl}, as described above (in Section 2.1.2), a grid search over flow-resistivity values was performed with flow-resistivity steps of 0.1 kNs/m^4 in the model. The best fit in terms of root-mean-square deviation (RMSD) between modelled and measured absorption coefficient values in the frequency range 160–2000 Hz, gave a best fit value of $\sigma = 22.5$ kNs/m^4 for the Miki model with hard backing.

The absorption coefficient values estimated from the measured data are shown in Fig. 2 together with the best fit model, with $\sigma = 22.5$ kNs/m^4. The model fitted in the frequency range 160–2000 Hz shows a good agreement with the absorption mean value from the measured data. It can be noted that the model predicts an increasing absorption at frequencies above 2.5 kHz, the validity of which cannot be substantiated by the measured data since they are not valid in that frequency range. Possibly the glass-fibre surface treatment of the absorber could impair the high-frequency absorption. In Fig. 3 the measured and modelled impedance values are plotted and the agreement is judged to be acceptable for both real and imaginary parts. The real part is seen to be positive for all frequencies, corresponding to a passive element, as expected, and the negative imaginary part (tending to zero at higher frequencies) corresponds to a spring-like impedance, as expected. In Fig. 4 the real and imaginary parts of the modelled normalised admittance, which is input to the calculation of the spherical reflection factor, are plotted over a wider frequency range.

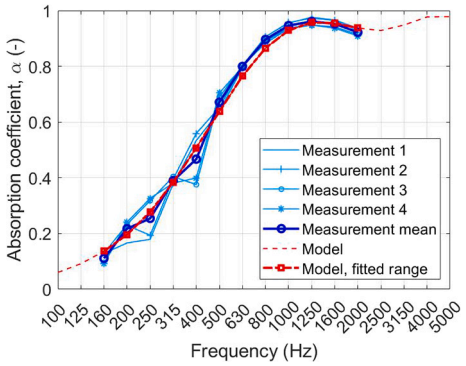

Fig. 2. Absorption coefficient values from four measurements with 50 mm samples and their mean value plotted together with the best fit model.

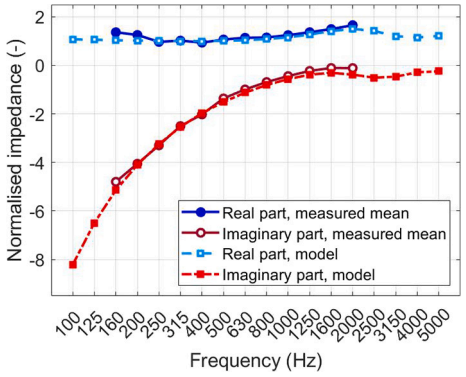

Fig. 3. Measured and modelled impedances for the 50 mm thick absorber.

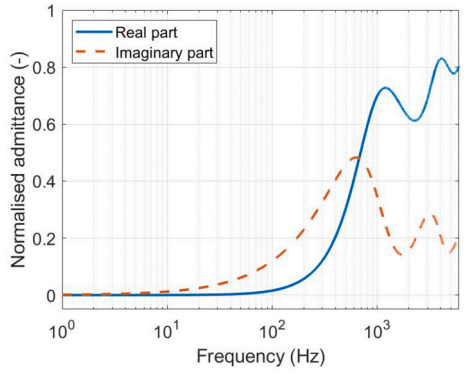

Fig. 4. Modelled normalised admittance for the 50 mm thick absorber.

An additional measurement using the impedance tube was made for 100 mm absorber thickness by placing two 50 mm thick samples on top of each other, with hard backing. In Fig. 5 it can be seen that the agreement between measured and modelled absorption is generally good also for 100 mm absorber thickness. However, at 400 Hz the measured absorption significantly exceeds that of the model. The cause for this is uncertain, but might be due to a thin air layer between the two mineral wool layers.

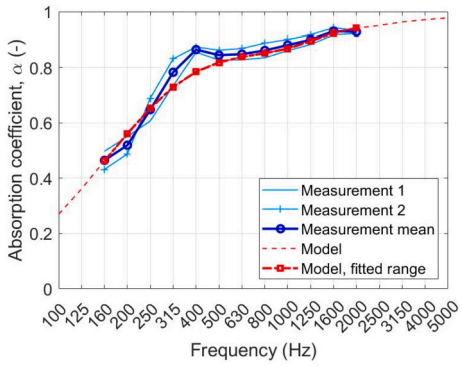

Fig. 5. Absorption coefficient values from two measurements with 100 mm samples and their mean value plotted together with the best fit model for 100 mm absorber thickness.

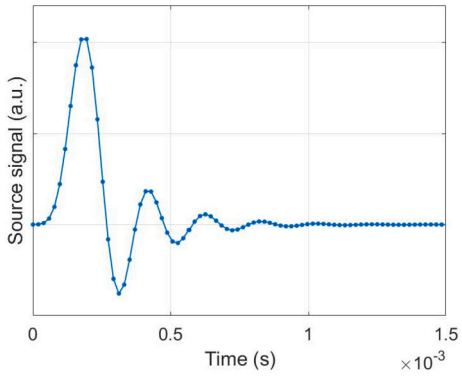

Fig. 6. Plot of source signal during first 1.5 ms.

2.1.4. Time-domain modelling

The sound pressure due to a direct and a reflected wave from a point source may be formulated in frequency domain as

$$G(\omega) = \frac{e^{-jk_0R_1}}{4\pi R_1} + Q\frac{e^{-jk_0R_2}}{4\pi R_2} \quad (12)$$

where the spherical reflection factor, Q, is described in Section 2.1.1 and the geometry is shown in Fig. 1. The formulation for $G(\omega)$ can be seen as a Green's function or frequency response function with two terms: $G_1(\omega) = \frac{e^{-jk_0R_1}}{4\pi R_1}$ representing the direct sound and $G_2(\omega) = Q\frac{e^{-jk_0R_2}}{4\pi R_2}$ representing the reflected sound.

The functions $G_1(\omega)$ and $G_2(\omega)$ are numerically transformed to time-domain signals $g_1(t)$ and $g_2(t)$ using an Inverse Fast Fourier Transform (IFFT). To do this, first the functions $G_1(\omega)$ and $G_2(\omega)$ are calculated at discrete steps, Δf, of the frequency, f (where $f = \omega/2\pi$), from zero frequency and up to half the sampling frequency (f_s). Secondly, the resulting spectra are tuned out at higher frequencies using a window function to avoid false ringing of the time signal. Thirdly, the now produced single-sided spectra of $G_1(\omega)$ and $G_2(\omega)$ together with their respective conjugate make up the double-sided spectra that are input to the IFFT, which gives the time signals $g_1(t)$ and $g_2(t)$ as output. The numerical implementation was made in Matlab. A time-domain sample rate of f_s =51.2 kHz with $N = 2^{18}$ samples were chosen and a Hann smoothing was used above 20 kHz. The step size in frequency is $\Delta f = f_s/N = 1/5.12 \approx 0.2$ Hz.

The signal, $s(t)$, emitted by the source is given by a delta function low-pass filtered with a cutoff frequency of $f_s/2$ using an 8th order Butterworth filter (see Fig. 6).

The functions $g_1(t)$ and $g_2(t)$ are convolved with the source signal, $s(t)$, to produce the pressure signals $p_1(t)$ and $p_2(t)$ at the receiver. Pressure signals are exemplified in Fig. 7 for the direct wave from the source, $p_1(t)$, and for the wave reflected in the absorber plane, $p_2(t)$; the example shows $p_2(t)$ for a rigid plane (hard surface with admittance $\beta = 0$), for a 50 mm porous absorber on hard backing and for a 100 mm porous absorber on hard backing.

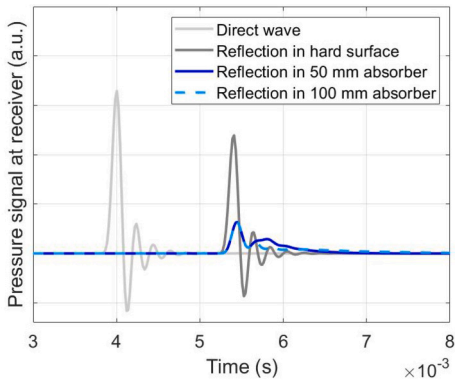

Fig. 7. Signals at receiver: Direct wave, wave reflected in a hard surface ($\beta = 0$), and wave reflected in a surface made up by a porous absorber with thickness 50 mm and 100 mm, following the Miki model with flow resistivity $\sigma = 22.5$ kNs/m^4 on hard backing (as described in Section 2.1.2).

2.1.5. Validation of the DFA model

A numerical validation test of the DFA model was made by moving the source and receiver to a large distance from the absorber surface (40 m and 20 m respectively) to resemble plane-wave condition. The calculated absorption coefficient as function of frequency showed indistinguishable results to those of the plane-wave absorber model in Fig. 2.

2.2. The SOPRA quick sound reflection index measurement method

2.2.1. Background

As mentioned in section 1, the SOPRA method can be applied to measure the sound reflection index of road noise barriers in-situ, i.e., in direct sound field. It is a simplified version of the European standard method EN 1793-5 [3], developed for enabling faster evaluations of installed noise barriers, but it cannot be used for declaring the acoustic performance of a noise barrier product. To not confuse it with the reflection index, RI, according to the EN 1793-5, the resulting quantity of this method is called the quick reflection index, RI_Q. The SOPRA method was part of the SOPRANOISE project [22], presented in a project report [9]. In an on-going research project, it was decided to test the SOPRA method (based on [9]) for collecting sound reflection data of installed noise barriers as well as of other surfaces in infrastructure environments. The execution and the results of the tests [23], led to the decision to use the method within the project. The methodology and the requirements for performing the quick sound reflection measurements can be found in [9] and also in [23], and in several published research articles [10–12]. The parts of the SOPRA method central to the current work are summarised below.

2.2.2. Quick sound reflection index measurements

To perform a sound reflection measurement of a noise barrier according to the SOPRA method, a portable loudspeaker and an array of 3–6 microphones are positioned in front of the noise barrier, see Fig. 8. A deterministic, flat-spectrum signal, e.g., pseudo-random noise, maximum-length sequence (MLS) or exponential sine sweep, is applied and the reflected sound pressure waves from the noise barrier are registered by the microphones. Reflections from surfaces further away, e.g. from the ground, will be excluded by time-windowing operations, as described in EN 1793-5 [3]. Repeating the measurement in free-field, in the same environment but without the noise barrier, gives the free-field impulse response, IR_{free}, which will be used for subtracting the direct component from the noise barrier's reflected impulse response

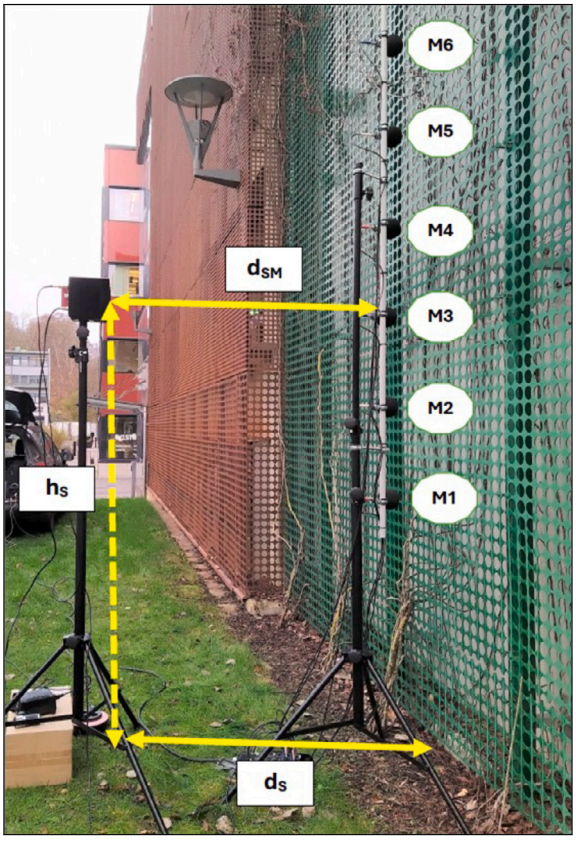

Fig. 8. The set-up for measuring the impulse response of the sound reflection.

IR_{refl}. The signal subtraction can for instance be made in Matlab, following the description in EN 1793-5 including the use of oversampling and least squares search for minimising the time difference between the two impulse response peaks.

Subsequently, the quick sound reflection index, RI_Q, can be calculated from (according to [9]):

$$RI_{Q,j} = \frac{1}{n_j} \cdot \sum_{k=1}^{n_j} \left[\frac{\int_{\Delta f_j} \left| F\left[h_{r,k}(t) \cdot w_{r,k}(t)\right] \right|^2 df}{\int_{\Delta f_j} \left| F\left[h_{i,k}(t) \cdot w_{i,k}(t)\right] \right|^2 df} \cdot C_{geo,k} \right]. \quad (13)$$

The variables in Eq. (13) are as follows:

$h_{i,k}(t)$ incident reference component of the free field impulse response at the k-th measurement point;

$h_{r,k}(t)$ reflected component of the impulse response taken in front of the sample under test at the k-th measurement point;

$w_{i,k}(t)$ time window (Adrienne temporal window, see [3]) for the incident reference component of the free field impulse response at the k-th measurement point;

$w_{r,k}(t)$ time window (Adrienne temporal window) for the reflected component at the k-th measurement point;

F symbol of the Fourier transform;

j index of the one-third octave frequency bands;

Δf_j width of the j-th one-third octave frequency band;

k microphone number according to Fig. 8;

n_j number of microphone positions on which to average;

$C_{\text{geo,k}}$ correction factor for geometrical divergence between the loudspeaker and the microphone position at the k-th measurement point, see [9].

Note that Eq. (13) is a simplified version of the expression to compute the reflection index RI according to the EN 1793-5.

The single-number rating of sound absorption under a direct sound field DL_{RIQ}, in decibel, is given by [9]

$$DL_{RIQ} = -10 \cdot \lg \left[\frac{\sum_{j=m}^{15} \text{RI}_{\text{Q},j} \cdot 10^{0.1 L_j}}{\sum_{j=m}^{15} 10^{0.1 L_j}} \right] \quad (14)$$

where the variables are as follows:

$RI_{Q,j}$ the quick sound reflection index, RI_Q, as a function of frequency, for the j-th one-third octave frequency band, according to Eq. (13);

m number of the lowest reliable one-third octave frequency band;

L_j relative A-weighted sound pressure levels (dB) of the normalised traffic noise spectrum, as defined in EN 1793-3 [24], in the j-th one-third octave band.

2.2.3. The measurement system

The electro-acoustic system for the SOPRA reflection measurement includes an electrical signal generator, a power amplifier and a loudspeaker, at least class 2 [25] microphones with amplifiers and with a maximum diameter of 1/2", input channels for 3–6 microphones and a signal analyser which can perform transformation between time and frequency domains. The measurements shall be made with a minimum sample rate of 44.1 kHz for analyses in the one-third octave bands between 200 and 5000 Hz. The signal-to-noise ratio, S/N, concerning the strength of the output sound signal in relation to the background noise shall be greater than 10 dB over the whole frequency range of the measurements. See [9] and EN 1793-5 for further requirements.

2.2.4. The measurement set-up

The measurement set-up, see Fig. 8, is the same for the reflection and the free-field measurements, the former placed in front of the noise barrier, with the distance $d_s = 1.5$ m between the loudspeaker and the reference plane[1] of the noise barrier. The centre of the membrane of the loudspeaker shall be at the reference height $h_s = 2.0$ m above the ground, which also is the height for microphone M_3, see Table 1. The microphones, mounted in a vertical array, are positioned between the loudspeaker and the noise barrier at the distance $d_M = 0.25$ m from the noise barrier (i.e., the distance between the loudspeaker front panel and microphone M_3 is $d_{SM} = 1.25$ m).
The heights of the microphones, mounted on a linear array, are listed in Table 1.

Microphones M_2, M_3 and M_4 are essential for the SOPRA reflection measurement. The possible use of additional microphones at larger heights, M_5 and M_6, depends on the height of the measured surface, which also determines the lowest reliable one-third octave band result of the measurements, see Table 2. Microphone M_1, at the lowest height, can be omitted since its impulse response is affected by the ground reflection and thus not included in the calculation of the quick reflection index, RI_Q.

Furthermore, it should be possible to arrange the microphone array so the distance between each microphone and the reference surface of

[1] The reference plane is formed by the most protruding parts of the noise barrier surface.

Table 1
Microphone heights above ground (the vertical spacing between the microphones on the array is 0.4 m).

Mic. nr.	Height (m)
M_1	1.2
M_2	1.6
M_3	2.0
M_4	2.4
M_5	2.8
M_6	3.2

Table 2
Microphones to be included for the calculation of the quick reflection index, Rl_Q, depending on the height of the measured noise barrier, h_B. The table is a shortened version of Table 5 in [9].

Barrier height, h_B (m)	Microphones	Lowest reliable 1/3-octave band
$h_B \leq 3$	$M_2 - M_4$	315 Hz
$3 < h_B \leq 5$	$M_2 - M_5$	250 Hz
$h_B > 5$	$M_2 - M_6$	200 Hz

the measured noise barrier is 0.25 m, i.e., whether the studied surface is vertical or inclined. In case of a concave or convex surface, the array shall be vertically positioned, with microphone M_3 at 0.25 m distance from the surface.

The free field measurement shall have the same set-up as the reflection measurement (except for the noise barrier) and be performed under the same conditions, in the same location. It must be set-up in a position where reflections from objects and other surfaces will be late enough to be excluded by the time-windowing operations of the impulse responses, as mentioned in Section 2.2.2.

2.2.5. Sample size and low frequency limit

According to EN 1793-5 for declaring the sound absorption performance of a certain product, the minimum dimension of a test sample required for the results being valid on the full frequency range of 200–5000 Hz is 4×4 m^2. However, smaller samples can be measured if the width of the analysis time window is adjusted for the smallest dimension (height or length) of the sample so that unwanted reflections are excluded. It must be noted though, that this causes a higher low-frequency limit, f_{min}, for the reflection index measurement, and the valid frequency range shall also be indicated in the single number value as $DL_{RIQ(f_{min}-5000\ \mathrm{Hz})}$.

3. Application of the DFA model for evaluating the in-situ SOPRA method

Section 3.1 describes a SOPRA quick sound reflection index (RI_Q) measurement of a wall fitted with a certain absorber. The DFA model is used to derive theoretical impulse responses based on an impedance model for the same absorber (see Section 2.1). The DFA impulse responses are subsequently entered into the SOPRA formula for calculation of the sound reflection index of the absorber. The single-number values, DL_{RIQ}, sound reflection indices, RI_Q, and impulse responses of the DFA model and the SOPRA measurement are compared in Section 3.2. If the results are similar, it is reasonable to assume that the SOPRA measurement results are valid. But if there are any significant differences between the DFA and SOPRA results, possible reasons for them should be examined.

3.1. Sound reflection index measurements with the SOPRA method

3.1.1. Test procedure

A test wall was constructed for the SOPRA measurement comprising 12.5 mm gypsum board on 11.0 mm OSB board mounted in a wooden frame. The surface under test had a dimension of 2.39×2.39 m^2, beginning 0.85 m above floor with a top height of 3.24 m above floor, see Fig. 9.

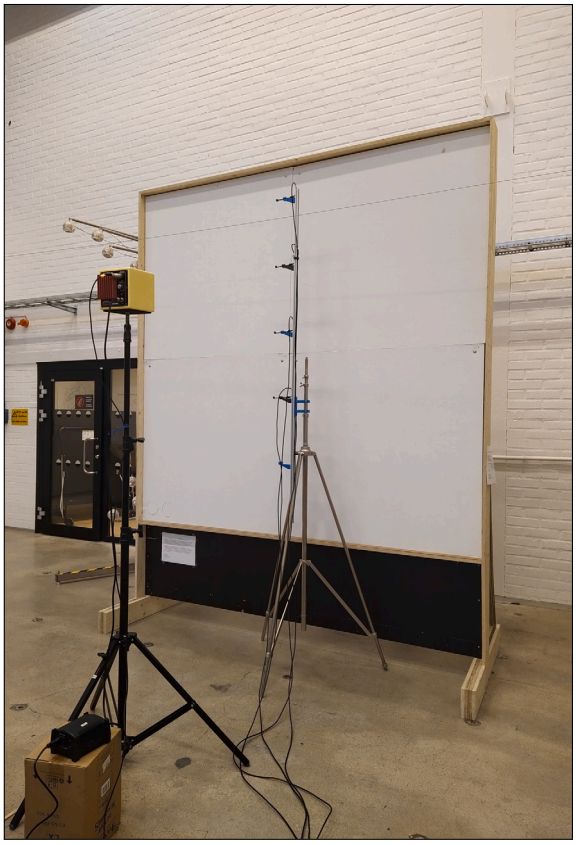

Fig. 9. The TA test wall with one layer of 50 mm absorber.

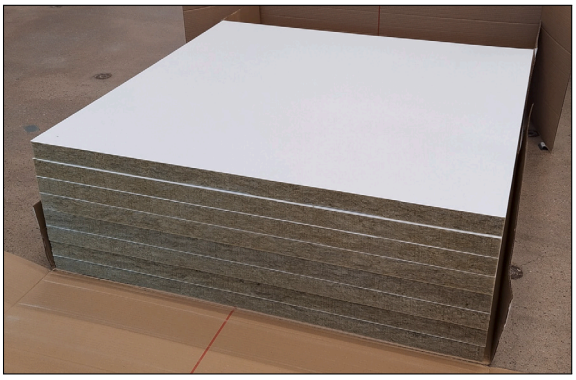

Fig. 10. The absorber sheets before mounting on the test wall.

The absorber, mounted on the test wall, was a 50 mm mineral wool sheet with a thin fibreglass sheet cover, Fig. 10.

The test wall was placed in a hall indoors, with the measured side far enough from other surfaces or objects to avoid parasitic reflections. A SQuadriga III [21] was used for the measurements. It is a compact mobile 24-bit recording and playback system with a signal generator, sound level meter function and a module for analysis of transfer function, coherence and impulse response. The resulting data were delivered as WAV files and in HEAD acoustics' hdf format. The hdf files were transformed into Matlab data files for further processing.

A pseudo random noise with flat spectrum was selected as source signal and emitted through a loudspeaker with integrated amplifier (Avantone Active Mix Cube). Four free-field microphones (G.R.A.S. 146

Fig. 11. Free field position.

AE 1/2" with integrated amplifiers) were placed 1.6–2.8 m above floor in the positions M_2–M_5 (Table 1). The measurements were made using a sample rate of 51.2 kHz for analysis in the one-third octave bands 200–5000 Hz.

The test wall was measured with two different absorber thicknesses:

- 50 mm absorber (1 layer) on top of the gypsum board, shown in Fig. 9.
- 100 mm absorber (2 layers) on top of the gypsum board.

The free field measurements were performed in the same hall with the same equipment and set-up between the loudspeaker and microphone antenna, see Fig. 11.

All measurements were performed twice, on two separate occasions, in October 2023 and in February 2024.

3.1.2. Measurement results

The acquired impulse response data from the sound reflection measurements were analysed according to the SOPRA method as described above. Even though the top of the test wall was at 3.24 m height, the lowest one-third octave band to consider in the calculations was 315 Hz, decided by the size of the absorber surface: 2.39×2.39 m^2 (see Table 2).

The resulting quick sound reflection indices, RI_Q, of the single microphones and averages were calculated according to Eq. (13) and presented in Fig. 12 (50 mm absorber) and Fig. 13 (100 mm absorber). Since microphone M_5 was quite close to the edge of the test wall and the IR, especially for the 50 mm absorber, appears to be affected by sound reflection/diffraction from the top edge of the wall, two different RI_Q averages are included in the figures, one based on the values of all microphones (M_2–M_5) and the other on M_2–M_4 only.

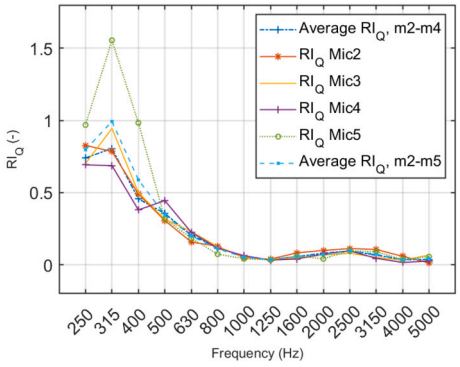

Fig. 12. RI_Q spectra for test wall with 50 mm absorber, for each microphone and for averages over microphones M_2–M_4 and M_2–M_5. Note: the valid measurement data starts from 315 Hz.

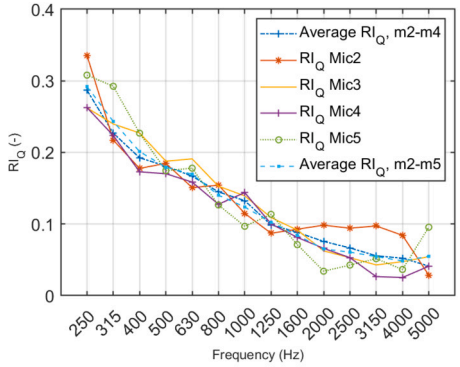

Fig. 13. RI_Q spectra for test wall with 100 mm absorber, for each microphone and for averages over microphones M_2–M_4 and M_2–M_5. Note: the valid measurement data starts from 315 Hz.

Table 3
The calculated single-number ratings of sound absorption, $DL_{RIQ(315-5000Hz)}$, measured in October 2023 and February 2024 on test wall with 50 and 100 mm thick absorber, as well as based on DFA model.

Absorber	Mics	Oct 23 DL_{RIQ} (dB)	Feb 24 DL_{RIQ} (dB)	DFA DL_{RIQ} (dB)
50 mm	M_2–M_4	8.1	8.2	8.1
	M_2–M_5	7.9	7.9	8.2
100 mm	M_2–M_4	9.1	9.1	9.0
	M_2–M_5	9.2	9.1	9.2

3.2. Comparisons of the DFA and SOPRA results

3.2.1. Comparison of the single-number ratings, DL_{RIQ}

As a first indication of the SOPRA measurement results, the calculated single-number rating for sound absorption, DL_{RIQ} (see Eq. (14)), can be informative. The $DL_{RIQ(315-5000Hz)}$ of both the DFA model and the SOPRA measurement are showing quite good agreement (a little less for the 50 mm absorber case if considering all microphones M_2–M_5 in the calculation of DL_{RIQ}), see Table 3. For the SOPRA measurement, DL_{RIQ} of the 50 mm absorber is 7.9–8.2 dB and 9.1–9.2 dB for the 100 mm absorber. The DFA model DL_{RIQ} of the 50 mm absorber is 8.1–8.2 dB, and 9.0–9.2 dB for the 100 mm absorber.

3.2.2. Comparison of the modelled and measured RI_Q spectra

The central part of the evaluation of the SOPRA measurement is the comparison of the modelled and measured sound reflection spectra. Thus, the DFA impulse response was entered into the SOPRA formula for the calculation of the reflection index and subsequently compared to the measured SOPRA reflection index. The results for both the 50 mm and 100 mm thick absorbers are plotted in Fig. 14.

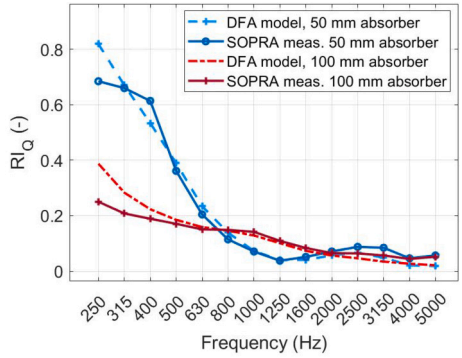

Fig. 14. Resulting RI_Q spectra from the DFA model and the SOPRA measurements, for 50 and 100 mm thick absorbers. Note: the valid measurement data starts from 315 Hz.

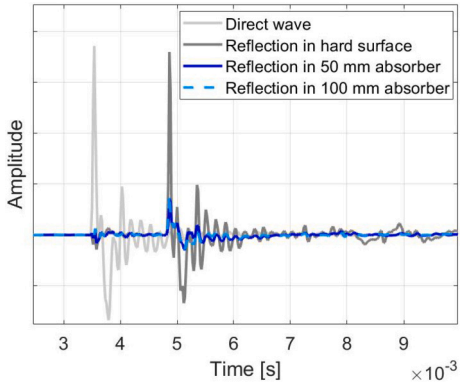

Fig. 15. Impulse responses of microphone 3 from SOPRA reflection measurement.

In Fig. 14 it can be observed that the one-third octave band values of the DFA model and the SOPRA measurement are quite similar from 500 Hz and up for both absorber thicknesses. It can also be seen that for the 100 mm absorber the DFA model results in higher RI_Q below 500 Hz than the measurement. Either the strength of the sound reflection is overestimated by the DFA model or underestimated by the measurement. Since the measurements are made on a finite surface while the DFA model assumes an infinite surface, it can be concluded that the sound reflection of the surface is overestimated by the DFA model relative to the measurement situation.

However, this is where an opportunity lies, if there otherwise is a good agreement between the reflection indices of the DFA model and the SOPRA measurement, the RI_Q of the DFA model could complement the measured RI_Q at lower frequencies, where measurements cannot deliver reliable results due to geometrical limitations. This could be useful for research purposes and possibly also for product development, but qualification of existing noise barrier products cannot be based on theoretical models.

3.2.3. Comparison of modelled and measured impulse responses

In the presented example, the measured impulse responses of M_3 (at the same height as the loudspeaker, i.e., normal incidence), shown in Fig. 15, did seem to be comparable with the theoretically obtained DFA impulse responses of the test wall's absorber material, previously described in Section 2.1 and illustrated in Fig. 7. However, it was noted that the measured IRs were approximately 0.4 ms earlier than the DFA IRs. The reason for this is unclear, but time differences between the modelled and measured impulse responses could originate from the measurement system or be an indicator of geometrical uncertainties, e.g., due to the acoustic centre of the loudspeaker. The possible impact on the final results of the measurements and of the modelling is judged to be small, whereby this deviation is not considered to be crucial for the conclusions of the current work.

3.2.4. Summary of comparisons of the DFA and SOPRA results

The results above show that comparison of the single-number ratings, DL_{RIQ}, is not enough for evaluating the quality of sound reflection index measurements; it also is necessary to study the RI_Q spectra of the DFA model and SOPRA measurement to increase certainty or to discover discrepancies, e.g., at lower frequencies. Furthermore, comparisons between modelled and measured impulse responses can reveal uncertainties of the measurements. Compensation for such uncertainties could increase the valid frequency range of the resulting RI_Q of the SOPRA measurement.

In general, it is advisable to apply the one-third octave band spectra, weighted according to the relevant traffic noise spectrum, when choosing or designing noise barriers or calculating the effect of absorbers for a specific site.

4. Conclusions and future work

This paper describes the development of the Direct Field Absorption (DFA) model, a time-domain model for the reflection of spherical waves in an absorber-like surface, and how the DFA model can be a valuable tool for evaluating the results of reflection index measurement methods like the SOPRA method. In addition to comparing final results, the model might be used to detect measurement anomalies and to study effects of geometrical uncertainties as well as background noise (the latter not addressed in this paper). These topics will be further investigated in future work, including the potential causes for the difference in arrival time between measured and modelled IRs.

The DFA model could also be useful for estimating the sound absorptive performance at lower frequencies of a noise barrier limited to its spatial extent in width and height, i.e., when it is physically impossible to measure. Moreover, it might be possible to use the DFA model to customise noise barriers (e.g., choose absorber) or to predict the performance of new designs of noise barriers. Further studies are necessary though, since the conclusions of this paper are based on only one kind of absorber.

CRediT authorship contribution statement

Monica Waaranperä: Writing – review & editing, Writing – original draft, Visualization, Software, Resources, Project administration, Methodology, Investigation, Formal analysis, Conceptualization. **Jens Forssén:** Writing – review & editing, Writing – original draft, Visualization, Supervision, Software, Resources, Methodology, Investigation, Formal analysis, Conceptualization.

Declaration of competing interest

The authors declare that they have no known competing financial interests or personal relationships that could have appeared to influence the work reported in this paper.

Data availability

Data will be made available on request.

Acknowledgement

The project is funded by the Swedish Transport Administration, project nr. 2020/26456.

References

[1] CEN, European Standard EN 1793-1:2017. Road traffic noise reducing devices - test method for determining the acoustic performance - part 1: Intrinsic characteristics of sound absorption under diffuse sound field conditions. Standard, CEN. 2017.

[2] CEN, European Standard EN 16272-1:2023. Railway applications - infrastructure - noise barriers and related devices acting on airborne sound propagation - test method for determining the acoustic performance - part 1: Intrinsic characteristics - sound absorption under diffuse sound field conditions. Standard, CEN. 2023.
[3] CEN, European Standard EN 1793-5:2016/AC:2018. Road traffic noise reducing devices - test method for determining the acoustic performance - part 5: Intrinsic characteristics - in situ values of sound reflection under direct sound field conditions. Standard, CEN. 2018.
[4] CEN, European Standard EN 16272-5:2023. Railway applications – infrastructure - noise barriers and related devices acting on airborne sound propagation - test method for determining the acoustic performance - part 5: Intrinsic characteristics - sound absorption under direct sound field conditions. Standard, CEN. 2023.
[5] CEN, European Standard EN 1793-2:2018. Road traffic noise reducing devices - test method for determining the acoustic performance - part 2: Intrinsic characteristics of airborne sound insulation under diffuse sound field conditions. Standard, CEN. 2018.
[6] CEN, European Standard EN 1793-6:2018+A1:2021. Road traffic noise reducing devices - test method for determining the acoustic performance - part 6: Intrinsic characteristics - in situ values of airborne sound insulation under direct sound field conditions. Standard, CEN. 2017.
[7] CEN, European Standard EN 16272-2:2023. Railway applications - infrastructure - noise barriers and related devices acting on airborne sound propagation - test method for determining the acoustic performance - part 2: Intrinsic characteristics - airborne sound insulation under diffuse sound field conditions. Standard, CEN. 2023.
[8] CEN, European Standard EN 16272-6:2023. Railway applications - infrastructure – noise barriers and related devices acting on airborne sound propagation - test method for determining the acoustic performance - part 6: Intrinsic characteristics - airborne sound insulation under direct sound field conditions. Standard, CEN. 2023.
[9] Garai M, Guidorzi P. SOPRANOISE deliverable D4.2. Report on the validation of the new quick methods in-situ with recommendations for proper use. Tech. Rep.; 2022.
[10] Guidorzi P, Garai M. A low-cost system for quick measurements on noise barriers in situ. IEEE Trans Instrum Meas 2022;71:1–14. https://doi.org/10.1109/TIM.2022.3218037.
[11] Garai M, Guidorzi P, Conter M, Fuchs A. SOPRANOISE: toward a quick measurement method to verify and monitor the acoustic performance of noise barriers on site. In: Proceedings of the international congress on acoustics; 2022.
[12] Conter M, Garai M, Clairbois JP, Fuchs A, Guidorzi P, Strigari F, et al. SOPRANOISE – a new quick method for measuring the acoustic quality of noise barriers in-situ. Transp Res Proc 2023;72:642–9. https://doi.org/10.1016/J.TRPRO.2023.11.450.
[13] Guidorzi P, Garai M. Sound insulation measurements on noise barriers across their entire extension: a preliminary study. In: Proceedings of 2020 international congress on noise control engineering; 2020.
[14] Chien CF, Soroka WW. Sound propagation along an impedance plane. J Sound Vib 1975;43(1):9–20. https://doi.org/10.1016/0022-460X(75)90200-X.
[15] Stinson MR. A note on the use of an approximate formula to predict sound fields above an impedance plane due to a point source. J Acoust Soc Am 1995;98(3):1810–2. https://doi.org/10.1121/1.413381.
[16] L'Espérance A, Nicolas JR, Herzog P, Daigle GA. Heuristic model for outdoor sound propagation based on an extension of the geometrical ray theory in the case of a linear sound speed profile. Appl Acoust 1992;37(2):111–39. https://doi.org/10.1016/0003-682X(92)90022-K.
[17] Kirby R. On the modification of Delany and Bazley fomulae. Appl Acoust 2014;86:47–9. https://doi.org/10.1016/j.apacoust.2014.04.020.
[18] Mechel FP. Design charts for sound absorber layers. J Acoust Soc Am 1988;83(3):1002–13. https://doi.org/10.1121/1.396045. Available from: https://pubs.aip.org/asa/jasa/article-pdf/83/3/1002/12233306/1002_1_online.pdf.
[19] Miki Y. Acoustical properties of porous materials-modifications of Delany-Bazley models. J Acoust Soc Jpn 1990;11(1):19–24. https://doi.org/10.1250/ast.11.19.
[20] ISO 10534-2:2023 – Acoustics – Determination of acoustic properties in impedance tubes — Part 2: Two-microphone technique for normal sound absorption coefficient and normal surface impedance. Tech. Rep. SIS (Swedish Standards Institute). Available from: https://www.iso.org/standard/81294.html.
[21] SQuadriga III (3324) datasheet: mobile recording and playback system - as a standalone system or USB front end. Tech. Rep. Available from: www.head-acoustics.de.
[22] CEDR. The european conference of directors of roads, research programme noise and nuisance. Available from: https://www.cedr.eu/peb-research-programme-2018-noise-and-nuisance, 2018.
[23] Waaranperä M, Forssén J, Kropp W. Measurement of sound reflection using the sopra method. In: Proceedings of forum acusticum; 2023.
[24] CEN, European Standard EN 1793-3:1997. Road traffic noise reducing devices - test method for determining the acoustic performance - part 3: Normalized traffic noise spectrum. Standard, CEN. 1997.
[25] IEC 61672-1:2013. Electroacoustics - sound level meters - part 1: Specifications. Standard, IEC. 2013.